

Eureka Journal of Physical and Chemical Research (EJPCR)

ISSN 2760-490X (Online)

Volume 2, Issue 4, April 2026



This article/work is licensed under CC by 4.0 Attribution

<https://eurekaooa.com/index.php/1>

THREE-DIMENSIONAL X-RAY TOMOGRAPHIC ANALYSIS OF SINGLE- AND BILAYER TiO₂ PHOTOANODES FOR DYE-SENSITIZED SOLAR CELLS

O. O. Mamatkarimov ¹,

S. S. Sharipbaev ¹

¹Namangan State Technical University,

160115, Namangan, Uzbekistan

E-mail: sharipbaev1999@gmail.com

ORCID 0009-0009-2269-7711

Abstract

Three-dimensional structural characteristics of TiO₂ photoanodes play a crucial role in determining the performance of dye-sensitized solar cells (DSSCs). In this work, single-layer and bilayer TiO₂ photoanodes were comparatively investigated using industrial microfocus X-ray tomography. The approach enabled volumetric visualization of internal architecture, thickness distribution, interfacial integrity, and defect formation not accessible by conventional two-dimensional techniques.

Tomographic analysis revealed that single-layer photoanodes exhibit a narrow, near-normal thickness distribution concentrated in the range of 0.030–0.055 mm with a peak around 0.048 mm, indicating high structural uniformity. Bilayer photoanodes demonstrated increased thickness variations, interfacial discontinuities, and higher probability of volumetric defects. These structural features correlate with extended electron transport pathways and

Eureka Journal of Physical and Chemical Research (EJPCR)

ISSN 2760-490X (Online)

Volume 2, Issue 4, April 2026



This article/work is licensed under CC by 4.0 Attribution

<https://eurekaopenaccess.com/index.php/1>

enhanced recombination losses. The results demonstrate that structural uniformity and interfacial integrity are decisive factors governing charge transport efficiency in TiO₂ photoanodes.

Keywords: Dye-sensitized solar cells; TiO₂ photoanode; X-ray tomography; Thickness uniformity; Structural defects; Charge transport

PACS: 88.40.jr, 81.70.Tx, 73.50.Pz, 68.55.-a

1. Introduction

Titanium dioxide (TiO₂) has been extensively employed as a photoanode material in dye-sensitized solar cells (DSSCs) owing to its high chemical stability, suitable energy band alignment, and large specific surface area for efficient dye adsorption. TiO₂-based photoanodes play a decisive role in governing light harvesting, electron transport, and recombination processes within DSSC devices [1–3]. The general structure of a typical DSSC is illustrated in Figure 1.

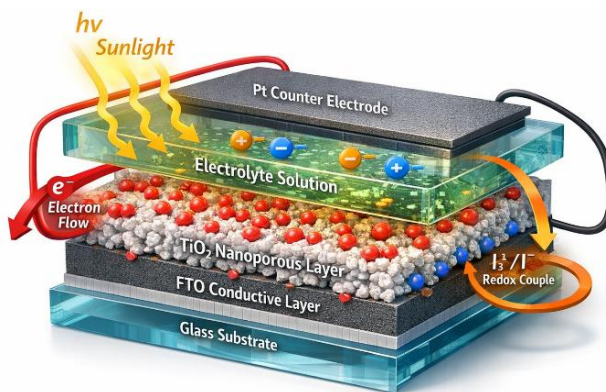


Figure 1. Schematic three-dimensional representation of a typical DSSC illustrating the main functional components: FTO glass substrate, nanoporous TiO₂ photoanode sensitized with dye molecules, electrolyte containing I³⁻/I⁻ redox couple, and platinum counter electrode.

Eureka Journal of Physical and Chemical Research (EJPCR)

ISSN 2760-490X (Online)

Volume 2, Issue 4, April 2026



This article/work is licensed under CC by 4.0 Attribution

<https://eurekaoa.com/index.php/1>

The TiO₂ photoanode thickness has been recognized as a critical parameter: increased thickness enhances dye loading and light absorption but simultaneously leads to prolonged electron transport pathways and increased recombination losses [4–7]. Consequently, the optimization of TiO₂ photoanode architecture has become a central research focus. Single-layer photoanodes remain widely investigated due to structural simplicity, with optimal thickness typically in the range of 30–45 μm, where a balance between dye adsorption and electron transport resistance is achieved. However, most studies rely on two-dimensional techniques such as SEM, providing limited insight into internal three-dimensional structure and thickness uniformity [8–11].

To address limitations of single-layer architectures, bilayer TiO₂ photoanodes combining nanoparticle-based photoactive layers with light-scattering layers have been proposed to improve photon utilization by increasing effective optical path length. These typically exhibit total thicknesses of 50–70 μm and enhanced photocurrent densities, but the introduction of internal interfaces increases structural complexity, non-uniform interlayer contact, charge transport resistance, and additional recombination pathways [11–13]. Structural characterization in such studies is predominantly based on SEM or AFM, which does not fully capture internal continuity of multilayer architectures.

Despite significant progress, comprehensive three-dimensional evaluation of TiO₂ photoanode internal structure remains largely unexplored. Industrial X-ray tomography offers a powerful approach for volumetric analysis, but its systematic application to comparative studies of single-layer and bilayer photoanodes has not been sufficiently reported [14]. This gap motivates the present work.

Eureka Journal of Physical and Chemical Research (EJPCR)

ISSN 2760-490X (Online)

Volume 2, Issue 4, April 2026



This article/work is licensed under CC by 4.0 Attribution

<https://eurekaopenaccess.com/index.php/1>

2. Materials and Methods

2.1. Preparation of TiO₂ photoanodes

Two photoanode configurations were analyzed: single-layer and bilayer TiO₂ structures deposited on glass substrates. The bilayer configuration consisted of two consecutively deposited TiO₂ layers, while the single-layer contained one functional layer. Rectangular samples with dimensions of approximately 10×20×3 mm, 13×20×3 mm, and 12×21×3 mm were prepared for tomographic investigation.

2.2. Tomographic characterization

Non-destructive structural characterization was carried out using a NanoVox-1000 microfocus X-ray tomography system. This technique provides volumetric information with micrometer-scale spatial resolution, enabling quantitative analysis of layer thickness, porosity, and interfacial integrity [15–17]. The method enables full-volume inspection without damaging samples and provides statistically representative structural information not obtainable from surface-based microscopy.

2.3. Thickness measurement and structural evaluation

Reconstructed tomographic datasets were analyzed to quantify TiO₂ layer thickness. For bilayer photoanodes, total thickness was 0.060–0.070 mm; for single-layer photoanodes, 0.050–0.055 mm. Measurements were performed at multiple locations. The analysis confirmed high precision of layer deposition, demonstrating the suitability of microfocus X-ray tomography for structural characterization of thin-film DSSC photoanodes [18–20].

Eureka Journal of Physical and Chemical Research (EJPCR)

ISSN 2760-490X (Online)

Volume 2, Issue 4, April 2026



This article/work is licensed under CC by 4.0 Attribution

<https://eurekaopenaccess.com/index.php/1>

3. Results

3.1. Tomographic visualization of TiO₂ photoanode architectures

Microfocus X-ray tomography enabled non-destructive three-dimensional visualization of TiO₂-based DSSC photoanodes. In bilayer photoanodes, two distinct TiO₂ layers were observed separated by a well-defined interfacial boundary (Figure 2). Single-layer photoanodes exhibited a continuous, homogeneous internal structure without internal interfaces (Figure 3), eliminating potential interlayer discontinuities.

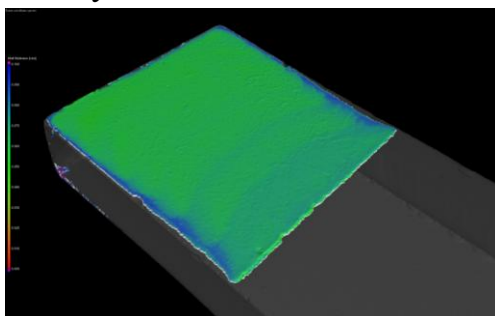


Figure 2. Three-dimensional tomographic reconstruction of the bilayer TiO₂ DSSC photoanode.

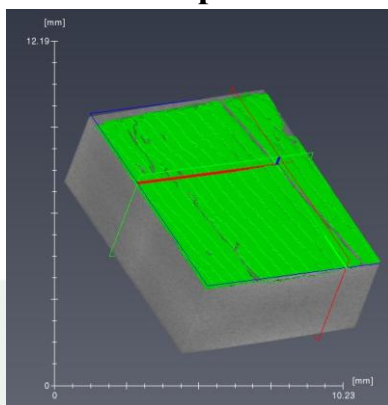


Figure 3. Three-dimensional tomographic reconstruction of the single-layer TiO₂ DSSC photoanode.

Eureka Journal of Physical and Chemical Research (EJPCR)

ISSN 2760-490X (Online)

Volume 2, Issue 4, April 2026



This article/work is licensed under CC by 4.0 Attribution

<https://eurekaopenaccess.com/index.php/1>

3.2. Thickness distribution and statistical analysis

Bilayer TiO_2 photoanodes showed total thickness of 60–65 μm , with local deviations reaching 70 μm (Figure 4). The average thickness was approximately 47.5 μm with a standard deviation of 7.9 μm . Single-layer photoanodes had average thickness of 50–55 μm with significantly narrower distribution (Figure 5).

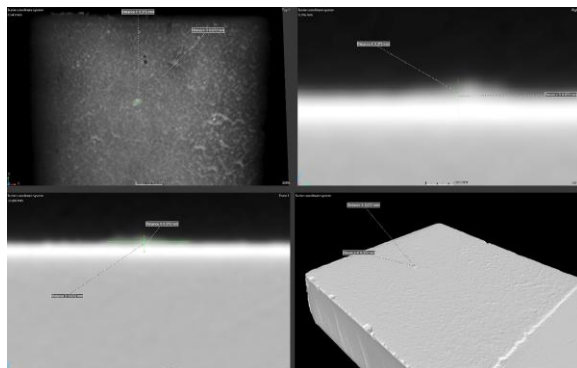


Figure 4. Tomographic cross-sections of bilayer TiO_2 photoanodes.

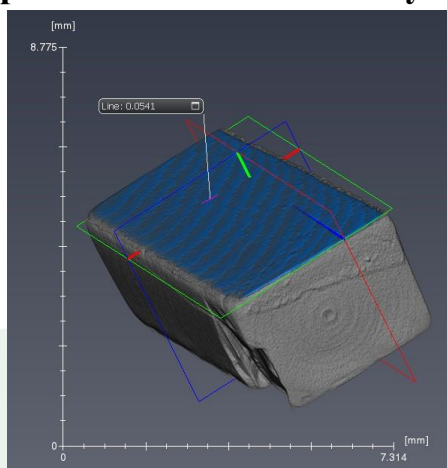


Figure 5. Tomographic cross-sections of the single-layer TiO_2 photoanodes.

Eureka Journal of Physical and Chemical Research (EJPCR)

ISSN 2760-490X (Online)

Volume 2, Issue 4, April 2026



This article/work is licensed under CC by 4.0 Attribution

<https://eurekaooa.com/index.php/1>

The wall thickness distribution of the single-layer photoanode (Figure 6) shows values concentrated within 0.030–0.055 mm with a peak at approximately 0.048 mm. The near-normal distribution suggests good uniformity and stability of the deposition process, beneficial for minimizing local variations in electron transport length.

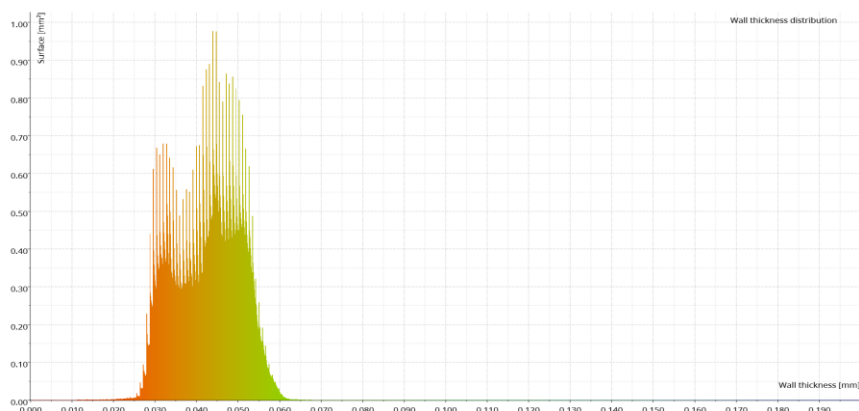


Figure 6. Wall thickness distribution of the single-layer DSSC photoanode. Thickness values concentrated in 0.030–0.055 mm with a peak around 0.048 mm.

Table 1. Structural parameters of TiO₂ photoanodes obtained by X-ray tomography

Parameter	Single-layer TiO ₂	Bilayer TiO ₂
Average thickness (μm)	40–45	50–55
Maximum thickness (μm)	~55	~70
Thickness uniformity	high	moderate
Internal interfaces	absent	present
Dominant structural feature	continuous layer	interlayer boundary

Eureka Journal of Physical and Chemical Research (EJPCR)

ISSN 2760-490X (Online)

Volume 2, Issue 4, April 2026



This article/work is licensed under CC by 4.0 Attribution

<https://eurekaoa.com/index.php/1>

3.3. Volumetric defects and pore formation

Tomographic inspection revealed isolated pores with depths of approximately 30 μm and diameters reaching 110 μm . Solid inclusions with dimensions of approximately 72 \times 345 \times 400 μm were also detected within the TiO₂ coating, locally disrupting photoanode continuity.

Table 2. Volumetric defects detected by X-ray tomography

Defect type	Characteristic size	Possible origin
Pore	$\varnothing \sim 110 \mu\text{m}$, depth $\sim 30 \mu\text{m}$	Trapped air bubbles
Solid inclusion	72 \times 345 \times 400 μm	Non-uniform mixing
Thickness gradient	up to $\sim 70 \mu\text{m}$	Deposition instability
Delamination zone	interface TiO ₂ /FTO	Weak interfacial adhesion

3.4. Interfacial integrity and delamination phenomena

Tomographic cross-sections revealed partial delamination between the TiO₂ layer and FTO glass substrate. The FTO layer thickness was approximately 21 μm , while the adjacent TiO₂ layer was approximately 27 μm . Delamination was predominantly observed in areas with pronounced thickness gradients and may adversely affect electron collection by increasing contact resistance.

3.5. Correlation between structural parameters and photovoltaic performance

Single-layer TiO₂-based DSSCs achieved power conversion efficiency up to 6.5%, whereas bilayer photoanodes exhibited approximately 2.8% under comparable conditions. The photovoltaic efficiency is defined as: $\eta = (J_{sc} \cdot V_{oc} \cdot FF) / P_{in}$, where J_{sc} is the short-circuit current density, V_{oc} is the open-

Eureka Journal of Physical and Chemical Research (EJPCR)

ISSN 2760-490X (Online)

Volume 2, Issue 4, April 2026



This article/work is licensed under CC by 4.0 Attribution

<https://eurekaopenaccess.com/index.php/1>

circuit voltage, FF is the fill factor, and P_{in} is the incident light power density ($100 \text{ mW} \cdot \text{cm}^{-2}$).

Table 3. Photovoltaic performance parameters of DSSCs

Configuration	Voc (V)	Jsc ($\text{mA} \cdot \text{cm}^{-2}$)	FF	η (%)
Single-layer TiO_2	0.693	9.53	0.538	6.5
Bilayer TiO_2	0.621	7.82	0.579	2.8

The improved performance of single-layer photoanodes correlates with enhanced thickness uniformity, absence of internal interfaces, and reduced defect density.

4. Discussion

The results provide three-dimensional structural evidence of how photoanode architecture influences DSSC performance.

4.1. Effect of photoanode thickness on charge transport and recombination

Photoanode thickness governs the balance between light harvesting and charge transport efficiency. Increasing TiO_2 thickness enhances dye adsorption and photocurrent generation but simultaneously increases electron transport resistance and recombination [4–6]. The tomographic results confirm that bilayer photoanodes exhibit larger thickness variations and local thickness maxima compared to single-layer structures, which may lead to extended electron transport pathways. Transport resistance increases with effective electron transport length: $R_{tr} \propto L/(\mu \cdot n \cdot q \cdot A)$, where L is photoanode thickness, μ is electron mobility, n is carrier concentration, q is elementary

Eureka Journal of Physical and Chemical Research (EJPCR)

ISSN 2760-490X (Online)

Volume 2, Issue 4, April 2026



This article/work is licensed under CC by 4.0 Attribution

<https://eurekaoa.com/index.php/1>

charge, and A is effective cross-sectional area. This is consistent with transport models by Bisquert and co-workers, who reported that prolonged electron diffusion lengths significantly enhance recombination probability in thick TiO_2 networks [15]. The improved thickness uniformity in single-layer photoanodes supports more homogeneous charge transport, reducing recombination losses and facilitating efficient electron collection at the FTO interface.

4.2. Role of internal interfaces in multilayer photoanodes

Multilayer and bilayer TiO_2 photoanodes have been explored to enhance light scattering and photocurrent density [10–11]. However, internal interfaces inevitably increase structural complexity. The present tomographic analysis reveals that internal interfaces in bilayer photoanodes are often associated with local discontinuities and adhesion imperfections difficult to detect using conventional techniques. Electrochemical impedance studies suggest that interlayer boundaries can act as recombination centers when electronic coupling between layers is insufficient [16–17]. Electron lifetime can be estimated as $\tau_n = 1/(2\pi f_{\max})$, where f_{\max} is the frequency corresponding to the maximum phase shift in the Bode plot. The three-dimensional visualization confirms that interface-related non-uniformities and imperfect interlayer contact are a plausible origin of reduced electron lifetime and increased recombination in multilayer DSSCs. The absence of internal interfaces in single-layer photoanodes eliminates these recombination-prone regions.

Eureka Journal of Physical and Chemical Research (EJPCR)

ISSN 2760-490X (Online)

Volume 2, Issue 4, April 2026



This article/work is licensed under CC by 4.0 Attribution

<https://eurekaoa.com/index.php/1>

4.3. Influence of pores and volumetric defects on DSSC performance

Porosity is essential for efficient dye loading in TiO₂ photoanodes; however, excessive or non-uniform porosity can introduce localized charge trapping sites and disrupt electron percolation pathways [7–9]. Tomographic data revealed the presence of large pores and solid inclusions with characteristic dimensions exceeding 100 μm, particularly in bilayer photoanodes. Unlike conventional SEM-based analyses providing limited local information, the applied tomographic approach enables volumetric quantification of defect size and spatial distribution. These results suggest that the increased number of deposition steps for bilayer architectures inherently raises the probability of defect formation, compromising structural reliability.

4.4. Interfacial adhesion and electron collection efficiency

The TiO₂/FTO interface is critical for electron collection. Tomographic visualization revealed localized delamination zones, particularly in regions with thickness gradients. Single-layer photoanodes exhibited fewer interfacial defects due to reduced mechanical stress, consistent with reports of improved electrical contact in simplified architectures [12–13, 18].

4.5. Advantages of three-dimensional tomographic analysis

This work demonstrates that industrial microfocus X-ray tomography provides critical insights into thickness uniformity, defect distribution, and interfacial integrity that cannot be obtained through conventional two-dimensional techniques [15–20]. The approach enables direct correlation between internal structure and photovoltaic performance, offering a valuable framework for rational optimization of DSSC photoanodes.

Eureka Journal of Physical and Chemical Research (EJPCR)

ISSN 2760-490X (Online)

Volume 2, Issue 4, April 2026



This article/work is licensed under CC by 4.0 Attribution

<https://eurekaoa.com/index.php/1>

5. Conclusion

A comprehensive structural investigation of single-layer and bilayer TiO₂ photoanodes for DSSCs was performed using industrial microfocus X-ray tomography. The applied non-destructive three-dimensional approach enabled direct visualization of internal layer architecture, thickness distribution, interfacial integrity, and volumetric defects not accessible by conventional two-dimensional characterization techniques.

Tomographic analysis revealed that single-layer TiO₂ photoanodes exhibit improved thickness uniformity, continuous internal structure, and reduced density of volumetric defects compared to bilayer architectures. In contrast, bilayer photoanodes demonstrated pronounced thickness gradients, internal interfacial discontinuities, and increased occurrence of pores and delamination zones, which may act as additional recombination pathways and increase charge transport resistance.

The detected structural differences provide a clear explanation for the superior photovoltaic performance of single-layer TiO₂-based DSSCs. The absence of internal interfaces, combined with improved interfacial adhesion to the FTO substrate, facilitates more efficient electron transport and charge collection. These findings indicate that structural uniformity and three-dimensional integrity are more critical for DSSC performance than increased architectural complexity. The presented approach provides valuable insights for the rational design and quality control of next-generation dye-sensitized solar cells.

Eureka Journal of Physical and Chemical Research (EJPCR)

ISSN 2760-490X (Online)

Volume 2, Issue 4, April 2026



This article/work is licensed under CC by 4.0 Attribution

<https://eurekaopenaccess.com/index.php/1>

References

1. O'Regan B., Grätzel M. A low-cost, high-efficiency solar cell based on dye-sensitized colloidal TiO₂ films. *Nature*, 353 (1991) 737–740.
2. Hagfeldt A., Boschloo G., Sun L., Kloo L., Pettersson H. Dye-sensitized solar cells. *Chemical Reviews*, 110 (2010) 6595–6663.
3. Zhang Q., Cao G. Nanostructured photoelectrodes for dye-sensitized solar cells. *Energy & Environmental Science*, 7 (2014) 253–267.
4. Boschloo G., Hagfeldt A. Characteristics of the iodide/triiodide redox mediator in dye-sensitized solar cells. *Accounts of Chemical Research*, 42 (2009) 1819–1826.
5. Wang Z.-S., Kawauchi H., Kashima T., Arakawa H. Significant influence of TiO₂ photoelectrode morphology on the energy conversion efficiency of N719 dye-sensitized solar cell. *Journal of Physical Chemistry C*, 112 (2008) 10691–10696.
6. Ito S., Murakami T.N., Comte P., Liska P., Grätzel C., Nazeeruddin M.K., Grätzel M. Fabrication of thin film dye sensitized solar cells with solar to electric power conversion efficiency over 10%. *Progress in Photovoltaics: Research and Applications*, 15 (2007) 603–612.
7. Wang X., Wang Y., Zhang L. Recent development of TiO₂ nanostructures for dye-sensitized solar cells. *Renewable & Sustainable Energy Reviews*, 147 (2021) 111220.
8. Kim H., Kim H., Lee J. Recent progress in dye-sensitized solar cells. *Materials Today Energy*, 21 (2021) 100786.
9. Zhang D., Li Q., Jiang J., Li X., Li Y. Influence of TiO₂ photoanode thickness on the performance of dye-sensitized solar cells. *Solar Energy*, 181 (2019) 445–452.

Eureka Journal of Physical and Chemical Research (EJPCR)

ISSN 2760-490X (Online)

Volume 2, Issue 4, April 2026



This article/work is licensed under CC by 4.0 Attribution

<https://eurekaoa.com/index.php/1>

10. Hore S., Vetter C., Kern R., Smit H., Hinsch A. Influence of scattering layers on efficiency of dye-sensitized solar cells. *Solar Energy Materials & Solar Cells*, 90 (2006) 1176–1188.
11. Yu H., Zhang S., Zhao H., Xue B., Liu P., Will G. High-performance TiO₂ photoanodes for dye-sensitized solar cells. *Applied Surface Science*, 527 (2020) 146780.
12. Ma X., Wang Y., Liu J., Zhang Z. Structural optimization of TiO₂ photoanodes for enhanced dye-sensitized solar cell performance. *Optical Materials*, 123 (2022) 111893.
13. Wang J., Liu Y., Zhang H., Li X. Structural and photoelectrochemical properties of TiO₂-based DSSCs. *Results in Physics*, 24 (2021) 104140.
14. Stock S.R. *MicroComputed Tomography: Methodology and Applications*. CRC Press, Boca Raton, 2009.
15. Maire E., Withers P.J. Quantitative X-ray tomography. *International Materials Reviews*, 59 (2014) 1–43.
16. Salvo L., Cloetens P., Maire E., Zabler S., Blandin J.J., Buffière J.Y., Ludwig W., Boller E., Bellet D., Josserond C. X-ray micro-tomography: an attractive characterisation technique in materials science. *Advanced Engineering Materials*, 5 (2003) 739–750.
17. Du Plessis A., Broeckhoven C., Guelpa A., le Roux S.G. Laboratory X-ray micro-computed tomography: a user guideline for biological samples. *GigaScience*, 6 (2017) 1–11.
18. Kastner J., Heinzl C., Requena G. X-ray computed tomography for non-destructive testing and materials characterization. *Materials Characterization*, 61 (2010) 1046–1055.

Eureka Journal of Physical and Chemical Research (EJPCR)

ISSN 2760-490X (Online)

Volume 2, Issue 4, April 2026



This article/work is licensed under CC by 4.0 Attribution

<https://eurekaooa.com/index.php/1>

19. Maire E., Buffière J.Y. 3D characterization of materials using X-ray tomography. *Metallurgical and Materials Transactions A*, 37 (2006) 1–16.
20. Withers P.J., Bouman C., Carmignato S., Cnudde V., Grimaldi D., Hagen C.K., Maire E., Manley M., du Plessis A., Stock S.R. X-ray computed tomography. *Nature Reviews Methods Primers*, 1 (2021) 18.